Intelligent Control and Automation, 2025, 16(3), 61-79
https://www.scirp.org/journal/ica
ISSN Online: 2153-0661
ISSN Print: 2153-0653

An Adaptive NF Technology for Bearing Condition Monitoring and Fault Diagnosis

Tahmid Delwar Toky, Ming Zhang, Wilson Wang

Department of Mechanical and Mechatronics Engineering, Lakehead University, Thunder Bay, Canada
Email: wilson.wang@Lakeheadu.ca

How to cite this paper: Toky, T.D., Zhang, M. and Wang, W. (2025) An Adaptive NF Technology for Bearing Condition Monitoring and Fault Diagnosis. *Intelligent Control and Automation*, **16**, 61-79.
https://doi.org/10.4236/ica.2025.163004

Received: July 6, 2025
Accepted: August 10, 2025
Published: August 13, 2025

Copyright © 2025 by author(s) and Scientific Research Publishing Inc.
This work is licensed under the Creative Commons Attribution International License (CC BY 4.0).
http://creativecommons.org/licenses/by/4.0/
Open Access

Abstract

Rolling element bearings are commonly used in rotating machines to transmit rotation and power. On the other hand, bearing faults could be the most common reason for machinery imperfections. Although many techniques have been proposed in the literature to detect bearing faults, each has its own merits and limitations, and none of them can perform reliable bearing fault detection and diagnosis. The objective of this work is to develop adaptive neurofuzzy (ANF) technology to integrate merits from several bearing fault detection techniques for automatic bearing condition monitoring and fault diagnosis. Three fault detection techniques are selected to extract representative features: envelope spectrum analysis, wavelet energy transformation, and variable mode decomposition. The feature indices will be the inputs to the proposed ANF classifier. The ANF can first classify if the bearing is healthy or faulty. If a fault is present, it can predict the type of bearing fault present in the signal, such as defect on the outer race, inner race or rolling element. A new training method is proposed to improve classification convergence and training efficiency. Its effectiveness is examined experimentally.

Keywords

Fault Diagnosis, Neurofuzzy Classification, Rolling Element Bearings, Machine Condition Monitoring, Signal Processing, Constrained Training

1. Introduction

Rolling element bearings are commonly used in rotating machines, such as automobiles, wind turbines, and motors, to support rotating shafts with less frictional torque. Based on investigation, up to 75% of imperfections in small and medium size machines are related to bearing defects [1] [2]. Reliable and real-time diagnostic information is very useful to machinery equipment for: 1) condition mon-

itoring to provide alarms before a fault reaches critical levels so as to prevent machine performance degradation, and improve production quality and safety; 2) schedule of repairs and maintenance operations without periodically shutting down machines for manual inspection so as to reduce operation expenses. 3) Maintenance costs can be further reduced in repairs by quickly identifying the damaged parts without routinely examining all the components involved in a machine.

Machine condition monitoring consists of two sequential processes: feature (symptom) extraction and decision-making (diagnosis). Feature extraction is a signal processing step to extract representative features from the measured signal, and decision-making is a process of classifying the extracted features into different machine health related categories for machine fault diagnosis. Although many signal processing techniques have been proposed in literature to detect faults in bearings, each technique has its own merits and limitations, and can be useful under specific bearing dynamics and operating conditions [2] [3]. The authors' research team has also proposed several bearing fault detection techniques using different approaches [3]-[6]. According to the authors' prior investigation, currently well-accepted bearing fault detection techniques include the envelope spectrum analysis (ESA) [7], wavelet energy transformation (WET) [3] and variable mode decomposition (VMD) [6]. A brief analysis of these three techniques will be given in Section 2.

Diagnostic decision-making is a process of classifying the obtained features into different bearing health-related categories. Its purpose is to integrate the merits of the selected signal processing techniques to make automatic and real-time machine fault diagnosis. The currently available automatic decision-making schemes can be classified as mathematical model-based methods and artificial intelligence (AI)-based techniques [8] [9]. AI-based diagnosis is employed in this study, because an accurate numerical model is difficult to derive especially in uncertain and noisy environments of rotating machines. AI-based diagnostic classifications can be conducted based on neural networks and fuzzy logic [10]-[12]. In order to overcome the limitations and reap the benefits of both neural networks and fuzzy systems, more interest has been paid to the use of synergetic schemes such as neural fuzzy levels [11]. The authors' research team has also proposed several AI classifiers for machine condition monitoring using techniques such as neural fuzzy and evolving clustering methods [13] [14]. However, these classical tools lack transparency and interpretability in reasoning. Although some deep-learning tools have been used for decision-making processes in recent years [15]-[17], these models are opaque to users, and it is difficult to explain the reasoning processes and to implement new knowledge to improve processing reliability.

The objective of this paper is to develop an automatic adaptive neuro-fuzzy (ANF) technology for more reliable bearing condition monitoring and fault diagnosis. The novelty aspects of this paper include: 1) The new ANF takes transparent and interpretive diagnostic reasoning for real-time bearing health condition mon-

itoring and diagnosis. The diagnostic knowledge from the expertise and online/offline learning can be incorporated into the fuzzy classification processes. 2) Three input features are extracted using the related signal process techniques of ESA, WET and VMD. The ANF technique can integrate merits of these selected features for more reliable fault detection. 3) A new constrained machine learning method is proposed to improve the adaptive capability and convergence of the ANF. The effectiveness of the developed ANF technology is verified by experimental tests.

The remaining of this paper is organized as follows: The related features for the inputs of ANF are briefly discussed in Section 2. The proposed ANF and the related training algorithm are discussed in Section 3. The effectiveness of the developed ANF monitoring technology is verified in Section 4 using experimental tests.

2. Bearing Fault Detection and Monitoring Indices

Bearing fault detection can be performed by using different signal carries such as vibration, electric current, noise, and lubricant. However, vibration signals provide the best signal-to-noise ratio, which will be used in this work.

Bearing fault detection remains a challenging task in this research and development field. Different from a mechanical component like a gear or shaft, a bearing is a system consisting of an outer race, an inner race, rolling elements and a cage, as illustrated in **Figure 1**. Even if a bearing is healthy, it generates vibration when discrete rolling elements pass through the load zone in sequence. Therefore, the bearing dynamics vary as the shaft/inner ring rotates. Any imperfection on the surface of a bearing component (*i.e.*, inner ring, outer ring, rolling element) will create extra impacts, which will then generate resonances on other bearing components and bearing support structures at particular frequencies. Thus, frequency analysis plays the key role in bearing fault detection and diagnosis [3].

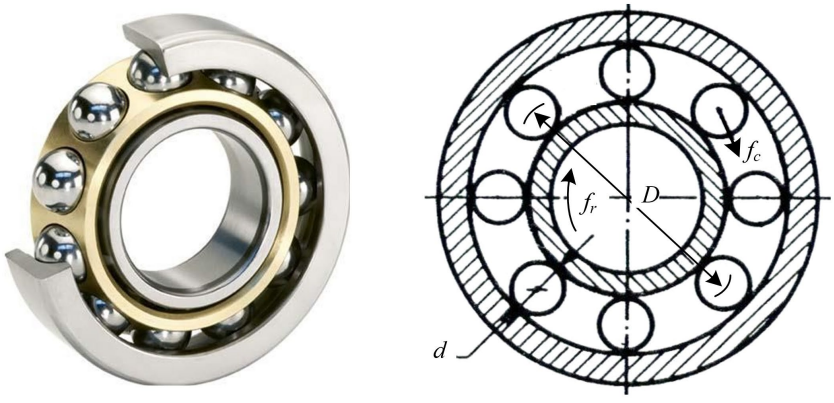

Figure 1. Structure of a rolling element (ball) bearing.

The bearing fault characteristic frequencies can be derived based on bearing dynamics analysis [3]. Consider a ball bearing as illustrated in **Figure 1**, with the ball diameter d, the pitch diameter D, the contact angle θ, and the number of roll-

ing elements Z. If the outer race is fixed and the inner race rotates at f_r Hz with the shaft, the characteristic frequencies for bearing outer race defect f_{od}, inner race defect f_{id}, and rolling element defect f_{rd} can be calculated as

$$f_{od} = \frac{Z}{2}\left(1 - \frac{d}{D}\cos\theta\right) \times f_r \tag{1}$$

$$f_{id} = \frac{Z}{2}\left(1 + \frac{d}{D}\cos\theta\right) \times f_r \tag{2}$$

$$f_{rd} = \frac{D}{d}\left(1 + \frac{d^2}{D^2}\cos^2\theta\right) \times f_r \tag{3}$$

As discussed in Introduction, there are many techniques in the literature that can be applied for bearing fault detection, which can be classified in time-, frequency- and time-frequency domain analysis methods. In time domain analysis, the fault detection is mainly based on the analysis of statistical parameters such as kurtosis and crest factor. Although the calculation of these statistical quantities is simple, however, these parameters are usually sensitive to bearing dynamics and operating conditions [18]. Direct frequency domain analysis methods, such as the Fourier transform (FT) and its relevant methods, are mainly used for stationary signal analysis; however, they may not be useful for processing time-variant or non-stationary signals that are often associated with machine defects [19]. Non-stationary signal properties can be analyzed in both the time and the frequency domains simultaneously to reveal transient features in a signal. Some common time-frequency domain techniques include the continuous/discrete wavelet transform, short-time FT, empirical mode decomposition, Hilber-Huang transform, etc. [20] [21].

Although many signal processing techniques have been proposed in the literature for bearing fault detection, each has its own merits and limitations in applications. From systematic analysis, three promising techniques will be selected for feature extraction and bearing fault detection: ESA [7], WET [3], and VMD analysis [6]. Details of these three techniques can be found from the related references. Some examples will be used for illustration on how to use these techniques for bearing fault detection.

Figure 2 shows the experimental setup used in this test. It is driven by a 3 HP induction motor operating at speeds ranging from 60 rpm (*i.e.*, 1 Hz) to 4,200 rpm (*i.e.*, 70 Hz), regulated by a frequency converter (VFD022B21A). To eliminate high-frequency vibrations from the drive motor, an elastic coupling is utilized in transmission. An optical sensor is used to provide a one-pulse-per-revolution to measure shaft speed. A static load is applied using two heavy mass discs. The variable dynamic load is provided by a brake system connected by a belt drive. The bearings (MBER-10K) under test are located on the left-side bearing housing, with bearing parameters listed in **Table 1**. Vibration signals are measured by using two accelerometers (ICP-603C01) mounted on the top and back of the bearing housing.

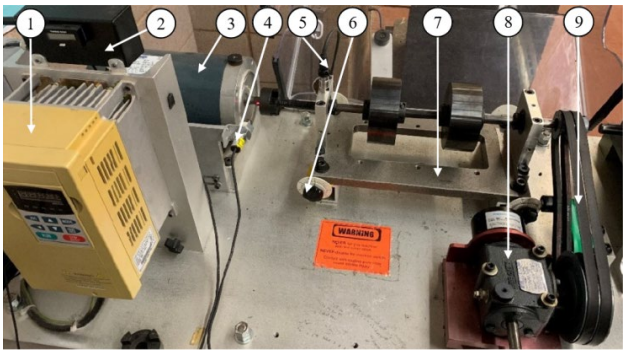

Figure 2. Experimental setup: 1) speed controller; 2) encoder display; 3) drive motor; 4) optical encoder; 5) ICP accelerometer; 6) misalignment adjustor; 7) adjustable rig; 8) variable load system; 9) belt drive.

Table 1. MBER-10K bearing parameters.

Bearing Components	Parameters
Pitch diameter D	33.503 mm
Rolling element diameter d	7.938 mm
Number of rolling elements (balls) z	8
Angle of contact θ	0°

Consider four data sets corresponding to a healthy bearing, and bearings with outer race defect, inner race fault and rolling element damage. If the shaft speed is 1,800 rpm or f_r = 30 Hz, with a medium load level, the characteristic frequency for a healthy bearing is f_r = 30 Hz. The characteristic frequencies for faulty bearings with defect on the outer race, inner race and rolling element can be calculated using Equations (1)-(3): f_{od} = 90.9 Hz, f_{id} = 147.9 Hz, f_{rd} = 91.57 Hz, respectively.

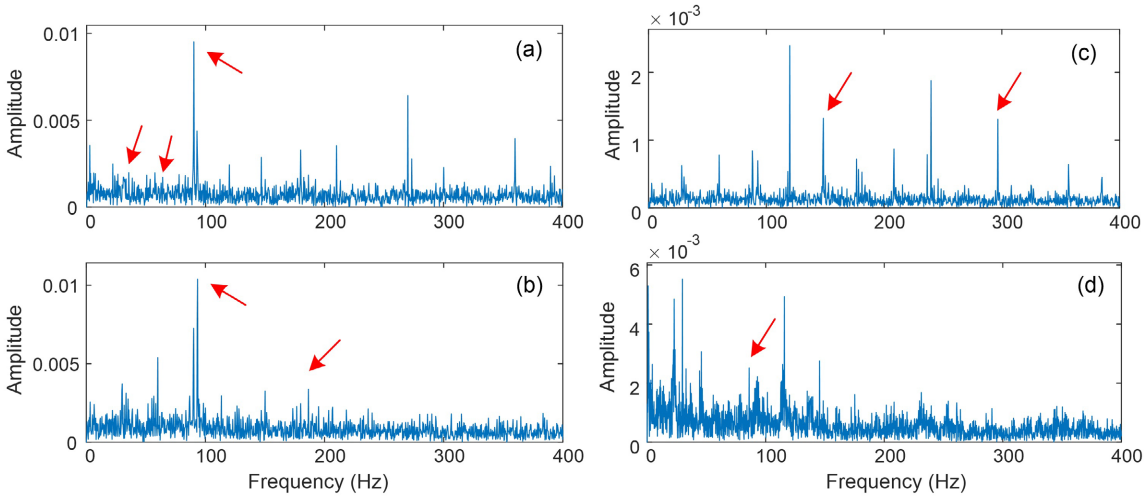

Figure 3. Fault detection results using the ESA technique: (a) for a healthy bearing (f_r = 30 Hz); (b) for a bearing with an outer race defect (f_{od} = 90.9 Hz); (c) for a bearing with an inner race defect (f_{id} = 147.9 Hz); (d) for a bearing with rolling element fault (f_{rd} = 91.57 Hz). (Arrows specify the associated characteristic frequencies and their harmonics).

Figure 3 shows the processing results using the ESA technique. For a healthy bearing in Figure 3(a), it can recognize the third harmonic (90 Hz) of f_r clearly, however, f_r and its second harmonic (60 Hz) cannot be recognized properly. For the bearing with an outer race damage in Figure 3(b), its characteristic frequency f_{od} = 90.9 Hz is too close to the third harmonic of the shaft speed (90 Hz), which can degrade the diagnostic accuracy. For the bearing with an inner race defect in Figure 3(c), although its characteristic frequency f_{id} = 147.9 Hz and its second harmonic can be recognized properly, their magnitudes don't domain the spectrum, which may result in false diagnosis. When the bearing has a ball fault, as seen in Figure 3(d), this ESA technique cannot clearly recognize the related characteristic frequency f_{rd} = 91.57 Hz because the fault feature is weak and modulated by other vibration signals.

Figure 4 shows the processing results using the WET technique. For a healthy bearing, it is seen from Figure 4(a) that WET cannot recognize the charactersitic frequency f_r (30 Hz), event though it can recognize the second harmonic (60 Hz) and third harmonic (90 Hz) that dominates the spectrum. For the bearing with an outer race damage in Figure 4(b), its characteristic frequency f_{od} = 90.9 Hz is also too close to the third harmonic of the shaft speed (90 Hz), which can degrade this fault diagnostic accuracy. For the bearing with an inner race defect in Figure 4(c), the characteristic frequency f_{id} = 147.9 Hz and its second harmonic can be recognized but they don't domain the spectrum, which may result in false diagnosis. On the other hand, as seen in Figure 4(d), this ESA technique fails to predict the bearing rolling element fault without recognizing the related characteristic frequency f_{rd} = 91.57 Hz.

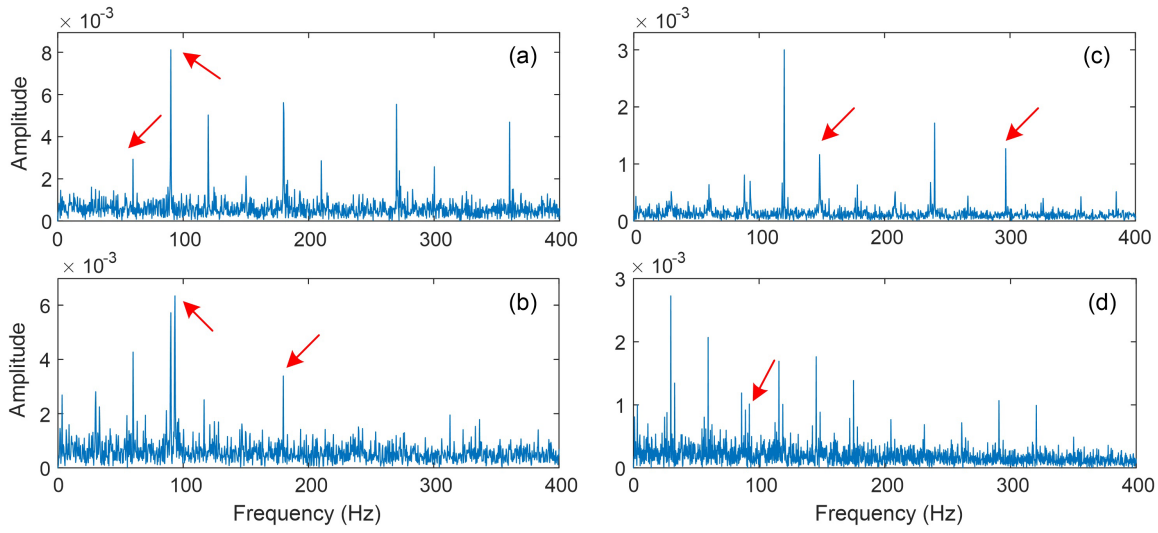

Figure 4. Fault detection results using the WET technique: (a) for a healthy bearing (f_r = 30 Hz); (b) for a bearing with an outer race defect (f_{od} = 90.9 Hz); (c) for a bearing with an inner race defect (f_{id} = 147.9 Hz); (d) for a bearing with rolling element fault (f_{rd} = 91.57 Hz). (Arrows specify the associated characteristic frequencies and their harmonics).

Figure 5 shows the processing results using the VMD technique. For a healthy bearing, it is seen in Figure 5(a) that, similar to the performance of the ESA and

WET techniques, the third harmonic of the characteristic frequency f_r (30 Hz) dominates the spectrum. For the bearing with an outer race damage in Figure 5(b), its characteristic frequency f_{od} = 90.9 Hz dominates the spectrum, which can provide clear fault diagnostic information. For the bearing with an inner race defect in Figure 5(c), the characteristic frequency f_{id} = 147.9 Hz and its second harmonic can be recognized clearly in this case, which also domain the spectrum. On the other hand, when a rolling element is damaged, it is seen from Figure 5(d) that this VMS technique can recognize the related characteristic frequency f_{rd} = 91.57 Hz, even though it does not dominate the spectrum, or the diagnostic accuracy is not high.

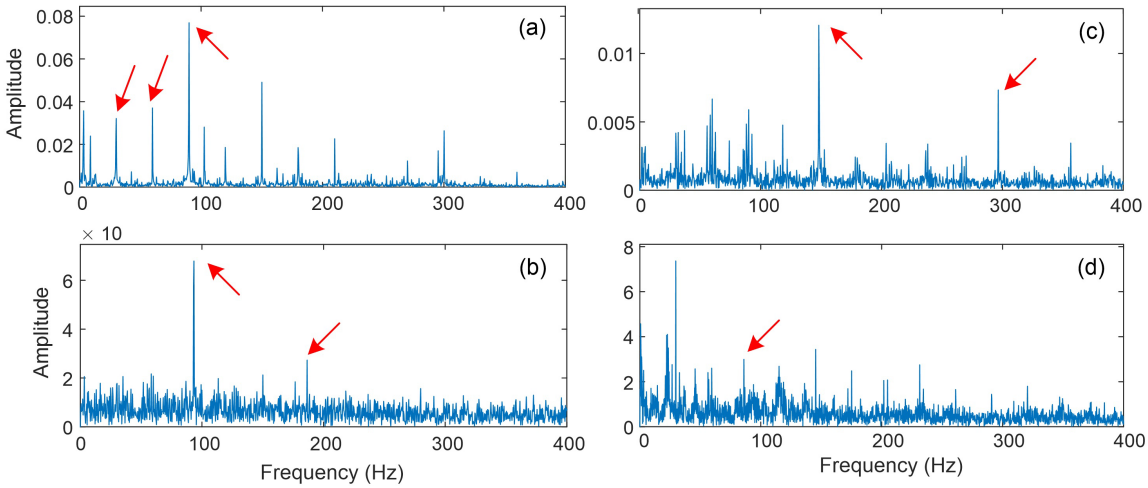

Figure 5. Fault detection results using the VMD technique: (a) for a healthy bearing (f_r = 30 Hz); (b) for a bearing with an outer race defect (f_{od} = 90.9 Hz); (c) for a bearing with an inner race defect (f_{id} = 147.9 Hz); (d) for a bearing with rolling element fault (f_{rd} = 91.57 Hz). (Arrows specify the associated characteristic frequencies and their harmonics).

It is seen that each technique has its own merits and limitations. The proposed ANF classifier aims to integrate the merits of three fault detection techniques to provide more reliable bearing health diagnosis, which will be discussed in the following section.

To quantify the obtained features as inputs to the ANF classifier, the output index is derived by

$$C_F = \frac{\sum_{f \in f_c} \left(A(f) / \max A(f) \right)}{\sum_{f} \left(A(f) / \max A(f) \right)} \tag{4}$$

where $A(f)$ is the spectral amplitude at frequency f, which is normalized by the maximum spectral amplitude around it; f_c denotes a bearing characteristic frequency and its first three harmonics.

3. ANF Classification Technique for Bearing Fault Diagnosis

The ANF classifier is developed to integrate the merits of the selected signal processing techniques of ESA, WET and VMD for automatic and more reliable bear-

ing health condition monitoring and fault diagnosis.

3.1. ANF Classification Structure

Figure 6 illustrates the network architecture of the proposed ANF classification technique. It has 6 layers, whose functions are discussed below.

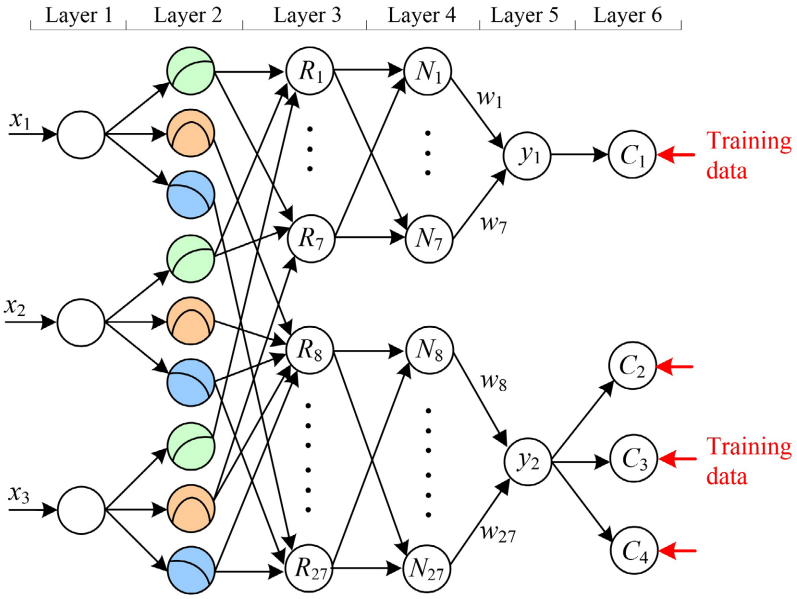

Figure 6. Architecture of the proposed ANF technique.

1) Layer 1: Layer 1 is the input layer. The input indices $\{x_1, x_2, x_3\}$ are derived from the selected fault detection techniques: ESA, WET and VMD.

2) Layer 2: This is the fuzzification layer. Each node in this layer is associated with a membership function (MF) for fuzzification of the input. Each input has three fuzzy sets representing "Small", "Medium" and "Large" MFs:

Sigmoid "Small" MFs: $\mu_{A,1}(x_i) = \dfrac{1}{1+\exp\left(-a_{i,1}\left(x_i - c_{i,1}\right)\right)}$; $a_{i,1} < 0$; $i = 1,2,3$. (5)

Gaussian "Medium" MFs: $\mu_{A_{i,2}}(x_i) = \exp\left(-\dfrac{\left(x_i - c_{i,2}\right)^2}{2\left(a_{i,2}\right)^2}\right)$, $i = 1,2,3$. (6)

Sigmoid "Large" MFs: $\mu_{A_{i,3}}(x_i) = \dfrac{1}{1+\exp\left(-a_{i,3}\left(x_i - c_{i,3}\right)\right)}$; $a_{i,3} < 0$; $i = 1,2,3$. (7)

where $c_{i,j}$ and $a_{i,j}$, $i = 1,2,3$ and $j = 1,2,3$, represent the respective center and the spread parameters of the MFs, which will be optimized in system training.

3) Layer 3: This layer performs fuzzy reasoning operations. With 3 inputs, each having 3 MFs, there are 27 fuzzy If-Then rules, formulated as:

$\Re_k$: If (x_1 is $A_{1,k}$) And (x_2 is $A_{2,k}$) And (x_3 is $A_{3,k}$) Then (Y is y_k) (with wight w_k), (8)

where $A_{i,k}$ represent MFs associated with rule $\Re_k$, $k = 1,2,\cdots,27$; $i = 1,2,3$;

w_k is the rule weight factor that is associated with the robustness of the diagnostic reasoning of the inputs in rule $\Re_k$. The diagnostic reasoning is conducted based on the following inferences:

i) If at least one inputs $\{x_1, x_2, x_3\}$ is Small, and the remaining inputs are Medium, then the bearing could be healthy with weights factors w_1 - w_7 for rules $\Re_1$ to $\Re_7$.

ii) Except the conditions in i), the rules from $\Re_8$ to $\Re_{27}$ are associated with the faulty condition with weight factors: w_8 - w_{27}.

If a max-product operator is used, the firing strength for the k^{th} rule T_k will be:

$$T_k = \mu_{A_{1,k}}(x_1)\mu_{A_{2,k}}(x_2)\mu_{A_{3,k}}(x_3), \quad k = 1,2,\cdots,27. \tag{9}$$

4) Layer 4: It is the normalization layer. The rule firing strength is computed as

$$U_k = \frac{T_k}{\prod_k T_k}, \quad k = 1,2,\cdots,7; \quad k = 8,9,\cdots,27. \tag{10}$$

5) Layer 5: It is the output layer. There are two nodes in this layer: y_1 is associated with the healthy bearing condition and y_2 is associated with faulty bearing condition. If centroid defuzzification is applied, the outputs will be:

$$y_1 = \frac{\sum_{k=1}^{7} U_k \times w_k}{\sum_{k=1}^{7} U_k} \tag{11}$$

$$y_2 = \frac{\sum_{k=8}^{27} U_k \times w_k}{\sum_{k=8}^{27} U_k} \tag{12}$$

6) Layer 6: This is the diagnostic classification layer. If $y_1 \in [0.50,1.00]$, the output corresponds to the healthy bearing condition C_1.

If $y_2 \in (0.50,1.00]$, the output corresponds to the faulty bearing condition. The fault type can be further classified into three categories:

If $y_2 \in (0.50,0.70]$, $y_2 \in C_2$: outer race bearing damage, which is the most common defect in bearing damage, because the fixed ring material is subjected to more fatigue loading.

If $y_2 \in (0.70,0.85]$, $y_2 \in C_3$: inner race bearing damage.

If $y_2 \in (0.85,1.00]$, $y_2 \in C_4$: rolling element bearing fault.

These category boundaries, 0.5, 0.7 and 0.85, are selected based on general reasoning. These category boundaries are fixed in training. After training, the related rule MF parameters and rule weights are adjusted and fit these categories.

3.2. Parameter Training

Once the ANF classifier is established, its parameters should be trained properly to improve classification convergence and adaptive capability. The ANF has both

linear and nonlinear parameters. The MF parameters in Layer 1 are nonlinear parameters, while the rule weight parameters are linear parameters. A new constrained training method will be proposed to train nonlinear parameters, and a recursive least squire estimator (RLSE), proposed by the authors' research team [22], will be adopted to update linear parameters.

Given a training data set $\left\{x_1^{(n)}, x_2^{(n)}, x_3^{(n)}; y_d^{(n)}\right\}$, where $y_d^{(n)}$ is the desired system output, $n = 1, 2, \cdots, N$; N is the total number of trinaing date paris. In training, if the bearing is healthy, $y_{1,d} = 0.75$. If the bearing is damaged, $y_{2,d} =$ 0.60, 0.80 and 0.90 corresponding to outer race, inner race and rolling element (ball) damage, respectively. The error function E can be formulated as:

$$E = \frac{1}{2}\sum_{n=1}^{N}\left[\left(y_1^{(n)} - y_{1,d}^{(n)}\right)^2 + \left(y_2^{(n)} - y_{2,d}^{(n)}\right)^2\right] \tag{13}$$

1) Constrained Training

A constrained training algorithm is proposed to update the fuzzy MF parameters in the ANF classifier. The purpose is to guarantee that a dominant rule always exists for fault diagnosis and that the associated degree of belief is greater than 50%. To achieve the 0.5-completeness, constraint functions are proposed next.

Consider the "Small" sigmoid MF $\mu_{A_{i,1}}(x_i) = \dfrac{1}{1+\exp\left(-a_{i,1}\left(x_i - c_{i,1}\right)\right)}$, $a_{i,1} < 0$, $i = 1, 2, 3$, and the Gaussian "Medium" MF: $\mu_{A_{i,2}}(x_i) = \exp\left(-\dfrac{\left(x_i - c_{i,2}\right)^2}{2\left(a_{i,2}\right)^2}\right)$. As illustrated in Figure 7, they intersect at point X_1. To ensure the minimum 50% of completeness in fault diagnostic reasoning, the following conditions must be satisfied at the crossover point X_1:

$$\frac{1}{1+\exp\left(-a_{i,1}\left(X_1 - c_{i,1}\right)\right)} = \exp\left(-\frac{\left(X_1 - c_{i,2}\right)^2}{2\left(a_{i,2}\right)^2}\right) \geq 0.5 \tag{14}$$

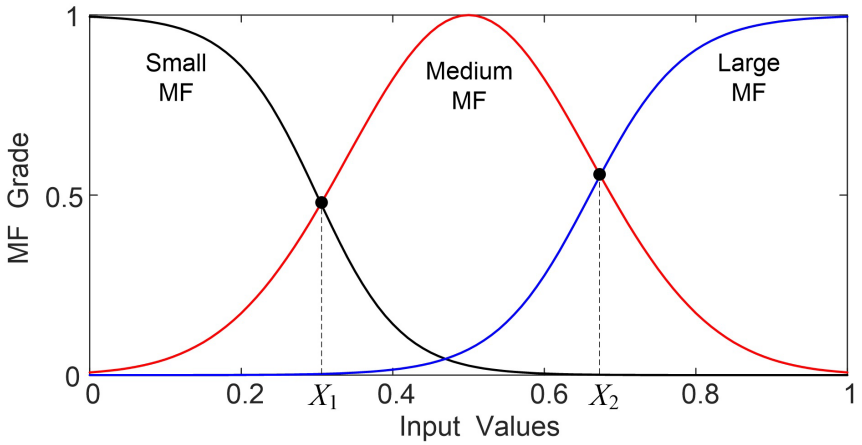

Figure 7. Constraint functions for parameter training.

Consider the "Large" sigmoid MF $\mu_{A_{i,3}}(x_i)=\dfrac{1}{1+\exp\left(-a_{i,3}\left(x_i-c_{i,3}\right)\right)}$, $a_{i,3}>0$, and the Gaussian "Medium" MF: $\mu_{A_{i,2}}(x_i)=\exp\left(-\dfrac{\left(x_i-c_{i,2}\right)^2}{2\left(a_{i,2}\right)^2}\right)$. As illustrated in Figure 7, they intersect at point X_2. To ensure the minimum 50% of completeness in fault diagnostic reasoning, the following condition must be satisfied at point X_2:

$$\exp\left(-\frac{\left(X_2-c_{i,2}\right)^2}{2\left(a_{i,2}\right)^2}\right)=\frac{1}{1+\exp\left(-a_{i,3}\left(X_2-c_{i,3}\right)\right)}\geq 0.5 \tag{15}$$

In training nonlinear system parameters of $a_{i,j}$ and $c_{i,j}$, $i=1,2,3$; $j=1,2,3$, for the n-th training step, these parameters can be updated by

$$a_{i,j}(n+1)=a_{i,j}(n)-\eta_a\frac{\partial E}{\partial a_{i,j}}, \tag{16}$$

$$c_{i,j}(n+1)=c_{i,j}(n)-\eta_c\frac{\partial E}{\partial c_{i,j}} \tag{17}$$

where η_a and η_c are update steps. Corresponding to the cross-over points X_1 and X_2, check if the minimum fuzzy completeness 50% can be satisfied from Equation (14) and Equation (15). If they can be satisfied, then keep the related parameters $a_{i,j}(n+1)$ and $c_{i,j}(n+1)$, $i=1,2,3$; $j=1,2,3$. Otherwise, $c_{i,j}(n+1)\Leftarrow c_{i,j}(n)$ and $a_{i,j}(n+1)\Leftarrow a_{i,j}(n+1)$, and proceed the following parameter training steps.

2) Linear Parameter Optimization

In linear parameter optimization, the nonlinear parameters remain fixed. Then the objective function (13) can be represented as $E(\boldsymbol{\theta}_n)$, where $\boldsymbol{\theta}_n=\left[w_1^{(n)},w_2^{(n)},\cdots,w_{27}^{(n)}\right]^{\mathrm{T}}$ at the current state n. The ANF output can be represented as

$$y_n(\boldsymbol{\theta}_n)=\boldsymbol{\Omega}_n^{\mathrm{T}}\boldsymbol{\theta}_n, \tag{18}$$

where $\boldsymbol{\Omega}_n$ is the resulting matrix from the corresponding fuzzy inference operation. The RLSE is computed by [22]

$$\boldsymbol{\theta}_{n+1}=\boldsymbol{\theta}_n+\boldsymbol{\Psi}_{n+1}\boldsymbol{\Omega}_n\left(d_n-\boldsymbol{\Omega}_n^{\mathrm{T}}\boldsymbol{\theta}_n\right) \tag{19}$$

$$\boldsymbol{\Psi}_{n+1}=\frac{1}{\alpha_n}\left[\boldsymbol{\Psi}_n-\frac{\boldsymbol{\Psi}_n\boldsymbol{\Omega}_n\boldsymbol{\Omega}_n^{\mathrm{T}}\boldsymbol{\Psi}_n}{\alpha_n+\boldsymbol{\Omega}_n^{\mathrm{T}}\boldsymbol{\Psi}_n\boldsymbol{\Omega}_n}\right] \tag{20}$$

where $n=0,1,\cdots,N-1$. α_n is a forgetting factor. The initial condition of the covariance matrix $\boldsymbol{\Psi}_n$ is $\boldsymbol{\Psi}_0=\rho\boldsymbol{I}$, where $\boldsymbol{I}$ is an identity matrix and ρ is a constant.

Detailed discussions of the RLSE method for linear parameter optimization can be found from [22].

3.3. Hybrid Training of ANF Parameters

A hybrid training strategy will be adopted in this work to improve training convergence and reduce trapping due to local minimums. In the forward path, nonlinear parameters are fixed, and linear parameters are updated using the RLSE method. In the backward path, the linear parameters are fixed and nonlinear parameters are updated using the proposed constrained training method. The training procedures are summarized below:

1) Initialize the parameters. By trials and errors, the initial system parameters are selected as $a_{i,j}=0.01$, $c_{i,j}=0.01$, $\eta_a=0.01$, $\eta_c=0.01$, $\alpha_0=0.995$, $\rho=1000$, $\boldsymbol{\theta}_0=\left[w_1^{(0)},w_2^{(0)},\cdots,w_{27}^{(0)}\right]^{\mathrm{T}}=\mathbf{1}$.

2) Input a training data set $\left\{x_1^{(n)},x_2^{(n)},x_3^{(n)};y_d^{(n)}\right\}$.

3) Compute the outputs $y_1^{(n)}$ and $y_2^{(n)}$ using Equation (11) and Equation (12).

4) Optimize linear weight parameters $\boldsymbol{\theta}_{n+1}$ using Equation (19).

5) Update nonlinear parameters using Equation (16) and Equation (17).

6) Check if the constraint functions (14) and (15) are satisfied. If they are, keep the updated parameters. Otherwise $c_{i,j}(n+1)\Leftarrow c_{i,j}(n)$ and $a_{i,j}(n+1)\Leftarrow a_{i,j}(n+1)$.

7) Calculate the training error $\Delta E=E(n+1)-E(n)$.

8) Repeat steps 2) to 7) until the training error goal (e.g., $\Delta E\le 10^{-5}$) is achieved, or the designated epoch number (e.g., 200) is reached.

On the other hand, after system training operations, some rule weight factors could become very small, for example, $w_k\le 1\%$ or 0.01. Then it means that these rules do not contribute much to the diagnostic classification processes. To facilitate the decision-making and machine learning processes, the low weight rules can be removed from the rule base.

4. Performance Verification

The effectiveness of the developed ANF classification technique will be examined experimentally in this section. Some related techniques will be used for comparison:

Table 2. Bearing characteristic frequencies at shaft speed.

Condition of the bearing	Characteristic frequencies in terms of f_r(Hz)
Healthy bearing	$f_H=f_r$
Outer race fault	$f_O=3.052\times f_r$
Inner race fault	$f_I=4.947\times f_r$
Rolling element fault	$f_B=3.983\times f_r$

ANFIS: the adaptive neural fuzzy inference system (ANFIS) from MATLAB will be used for comparison, which uses the same inputs and similar fuzzy reasoning

architecture as the ANF, but the training is based on classical gradient-LSE algorithms.

ANF-0: It has the same inputs and reasoning architecture as the ANF, but it uses the classical gradient-LSE training algorithms.

The datasets from Case Western Reserve University [23] are used for initial training of the ANFIS, ANF-0, and ANF classifiers. In total, 250 data sets are used for training: 80 for healthy bearings, 60 for bearings with outer face damage, 60 for bearings with inner race fault, and 50 for bearings with ball damage. 90 data sets are used to testing: 30 for healthy bearings, 20 for bearings with outer face damage, 20 for bearings with inner race fault, and 20 for bearings with ball damage.

These classifiers are then used for real-time bearing health condition monitoring in this test. The experimental setup is illustrated in **Figure 2**. The tested bearings are installed to the left bearing housing. Tested bearing parameters are listed in **Table 1**. For each of the bearing conditions (*i.e.*, health, outer race damage, inner race fault and rolling element damage), the load level changes from light (*i.e.*, 0.5 Nm), medium (2.0 Nm) to heavy (*i.e.*, 5.0 Nm). The motor speed, or bearing rotation f_r, varies between 120 rpm (*i.e.*, 2 Hz) and 3600 rpm (*i.e.*, 60 Hz). The related characteristic frequencies corresponding to different bearing conditions are listed in **Table 2** in terms of bearing speed (or motor speed) f_r.

4.1. Monitoring Results for a Healthy Bearing

Firstly, a healthy bearing is installed tested, with speed changes from 2 - 60 Hz, and load varies from light to heavy. Fifty test data sets are tested corresponding to different load (torque) and speed conditions. The diagnostic classification results using ANFIS, ANF-0 and ANF techniques are illustrated in **Figures 8-10**, respectively. The ANFIS classifier misclassifies 2 data sets from healthy state (C_0) to inner race damage state (C_2), due to quick load and speed changes. Both the ANF-0 and ANF generate 1 misclassification from the healthy state (C_0) to rolling element damage state (C_4), due to impacts caused by sudden load changes in the tested bearing.

4.2. Monitoring Results for a Bearing with Outer Race Defect

When the monitored bearing has outer race damage, over the 50 monitored data sets corresponding to variable bearing speeds changing from 2 - 60 Hz, and load varying from light to heavy, the ANFIS classifier generates 2 misclassifications from outer race damage state (C_1) to rolling element fault state (C_3). ANF-0 provides 1 misclassification also from outer race fault state (C_1) to rolling element damage state (C_3), over 50 test data sets. On the other hand, the proposed ANF technique generates no misclassifications in this case. It is relatively easier to detect outer race defects, as the damage related impact features do not vary with time. Most vibration-based fault detection techniques could recognize the bearing defect.

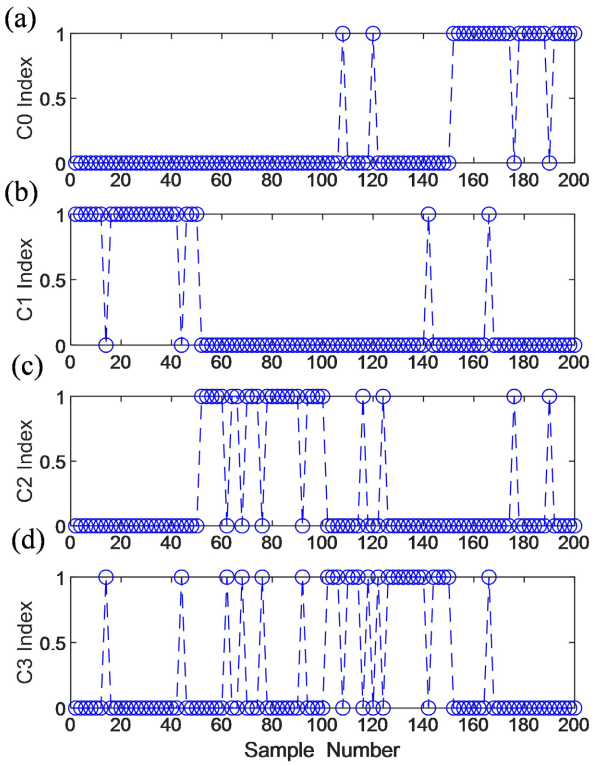

Figure 8. Diagnostic outputs of the ANFIS classifier: (a) for a healthy bearing; (b) for a bearing with outer race fault; (c) a bearing with inner race fault; (d) for a bearing with rolling element fault.

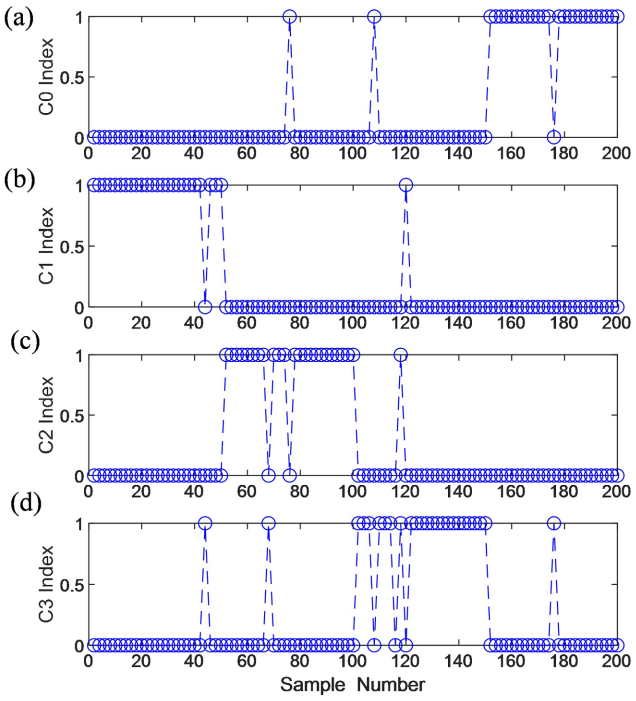

Figure 9. Diagnostic outputs of the ANF-0 classifier: (a) for a healthy bearing; (b) for a bearing with outer race fault; (c) a bearing with inner race fault; (d) for a bearing with rolling element fault.

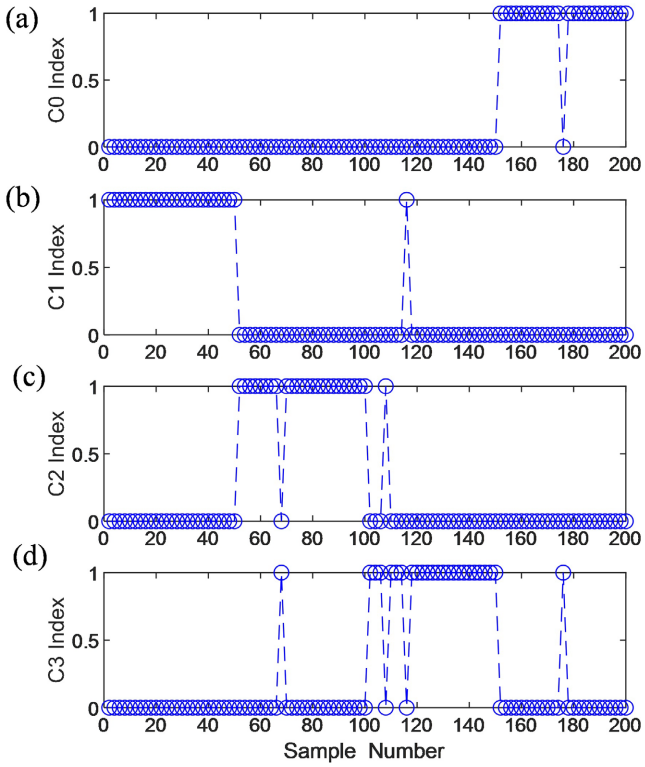

Figure 10. Diagnostic outputs of the ANF classifier: (a) for a healthy bearing; (b) for a bearing with outer race fault; (c) a bearing with inner race fault; (d) for a bearing with rolling element fault.

4.3. Monitoring Results for a Bearing with Inner Race Defect

In monitoring of a bearing with inner race fault, over the 50 monitored data sets corresponding to variable bearing speeds from 2 - 60 Hz, and load varying from light to heavy, the ANFIS classifier generates 4 misclassifications, all from inner race damage class (C_2) to rolling element fault class (C_3) as both features are time-varying. The ANF-0 classifier generates 2 misclassifications: one from inner race fault (C_2) to healthy state (C_0), or the classifier misses the bearing inner race damage, and another one from inner race fault state (C_2) to rolling element fault state (C_3). The proposed ANF classifier provides only 1 misclassification in this case, from C_2 to C_3, which performs better than both the ANFIS and ANF-0 techniques.

4.4. Processing Results for a Bearing with Rolling-Element Defect

In the tests of bearing with rolling element (ball) defect, over the 50 monitored data sets corresponding to variable bearing speeds from 2 - 60 Hz, and load varying from light to heavy, the ANFIS classifier generates 5 misclassifications: missing 2 fault detections from C_3 to C_0, two from C_4 to C_3, and 1 from C_4 to C_2. The ANF-0 provides 3 misclassifications: one from C_3 to C_0 (or missed the fault detection), one from C_4 to C_3, and one from C_4 to C_2, respectively. The proposed ANF technique generates 2 misclassifications only: one from C_4 to C_3, and one from C_4 to C_2, respectively. As discussed in Section 2, it is usually more challenging to di-

agnose rolling element fault, because the fault-related representative features are time-varying due to slips among bearing components. In addition, these features are modulated by other strong vibration signals.

Table 3 summaries the overall diagnostic accuracy of the three classifiers. The proposed ANF technique outperforms the ANF-0 and ANFIS in accuracy (98.0% versus 96.5% and 93.5%), due to its more efficient reasoning and training operations.

Table 3. Comparison among three classifiers.

Classifiers	Missed Alarms	False Alarms	Accuracy
ANFIS Classifier	2	11	93.5%
ANF-0 Classifier	2	5	96.5%
ANF Classifier	0	4	98.0%

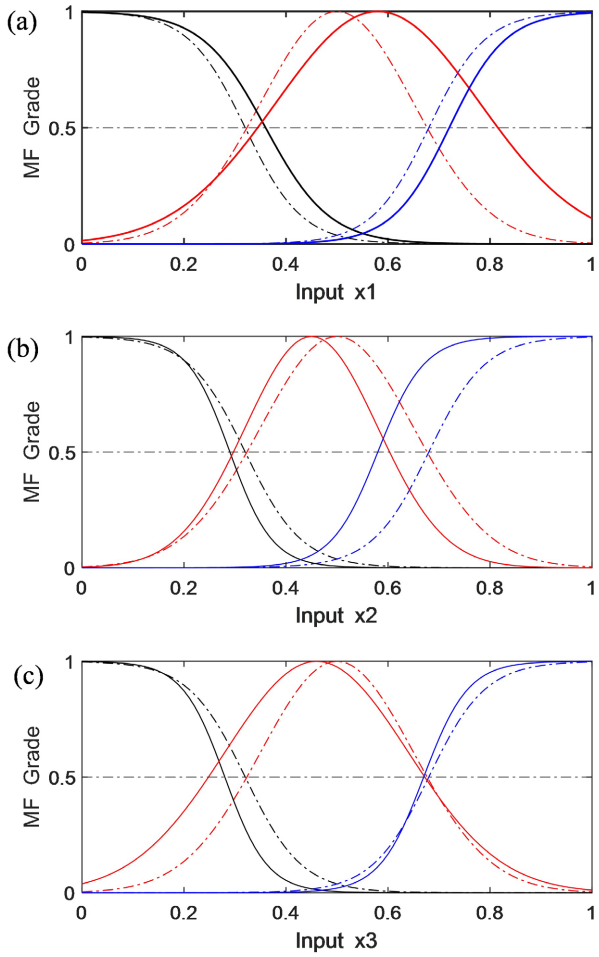

Figure 11. MF parameters before and after training operations: (a) x_1, (b) x_2, (c) x_3. Initial MFs (dashed lines); MFs after training (solid lines).

Figure 11 shows the initial and final MF parameters after real-time training. It is seen that the MFs after training are well managed with fuzzy completeness

greater than 50% (*i.e.*, 0.5). Consequently, the fuzzy reasoning accuracy and efficiency can be improved in comparison with the general gradient-LSE algorithms.

Figure 12 illustrates the fuzzy rule weight factors, with unity initial values. Three rules have weight factors of less than 0.01 (*i.e.*, 1%), due to over-mapping. These redundant rules will be removed from the following reasoning operations, which can reduce the rule base dimension and further improve the process efficiency, which is important for real-time machine condition monitoring application.

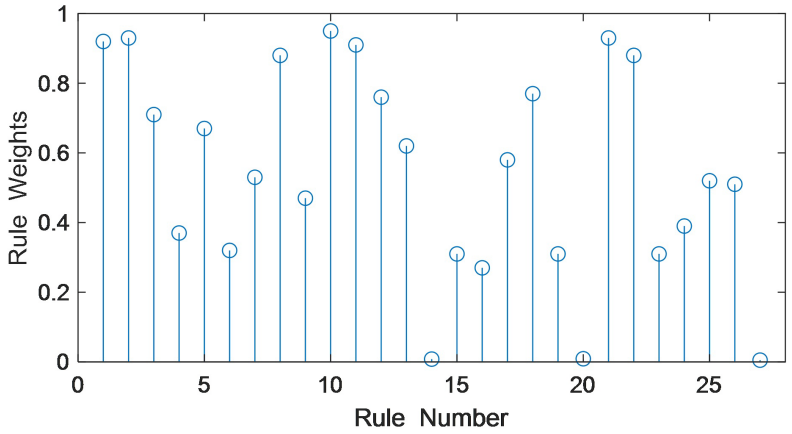

Figure 12. Rule weight factors after training, with unity initial weight factors.

5. Conclusion

Rolling element bearings are commonly used in rotating machines, while most rotating machine imperfections are related to bearing faults. On the other hand, it remains a challenging task to reliably predict bearing defects using available fault detection techniques. In this paper, an adaptive neuro-fuzzy, ANF, classification technology has been developed for bearing condition monitoring. Three features from the related fault detection techniques: ESA, WET and VMD, are selected and monitoring indexes are derived as inputs to the ANF. The ANF can integrate the merits of the selected fault detection techniques to provide more efficient bearing fault diagnosis. A new constrained learning method is proposed to update system parameters but retain sufficient fuzzy completeness (50%), to ensure there is at least one fuzzy rule dominating the pattern classification process. The ANF can first classify if the bearing is healthy or faulty. If a fault is present, the ANF can predict the type of bearing fault such as defect on the outer race, inner race or rolling elements. Its effectiveness has been verified by experimental tests corresponding to different bearing and test conditions. Test results show that the proposed ANF technique is a reliable and efficient bearing condition monitoring technology. It performs better than the related classification techniques. It has potential to be used for real-world machine condition monitoring and fault diagnosis applications.

Conflicts of Interest

The authors declare no conflicts of interest regarding the publication of this paper.

References

[1] Aysel, H.I., Cai, X. and Prugel-Bennettet, A. (2023) Multilevel Explainable Artificial Intelligence: Visual and Linguistic Bonded Explanations. *IEEE Transactions on Artificial Intelligence*, **5**, 2055-2066.

[2] Li, H., Wang, T., Zhang, F. and Chu, F. (2025) VMDPgram: An Effective Signal Decomposition Method for Rolling Bearing Fault Diagnosis. *IEEE Transactions on Instrumentation and Measurement*, **74**, Article ID: 3519010. https://doi.org/10.1109/tim.2025.3550998

[3] Wang, W. (2021) Analysis of Fault Detection in Rolling Element Bearings. *IEEE Instrumentation & Measurement Magazine*, **24**, 42-49. https://doi.org/10.1109/mim.2021.9436098

[4] Shukla, A., Mahmud, M. and Wang, W. (2020) A Smart Sensor-Based Monitoring System for Vibration Measurement and Bearing Fault Detection. *Measurement Science and Technology*, **31**, Article ID: 105104. https://doi.org/10.1088/1361-6501/ab8dfc

[5] Sun, S., Zhang, S. and Wang, W. (2023) A New Monitoring Technology for Bearing Fault Detection in High-Speed Trains. *Sensors*, **23**, Article 6392. https://doi.org/10.3390/s23146392

[6] Zhang, M., Xing, X. and Wang, W. (2024) Smart Sensor-Based Monitoring Technology for Machinery Fault Detection. *Sensors*, **24**, Article 2470. https://doi.org/10.3390/s24082470

[7] Kim, S., An, D. and Choi, J. (2020) Diagnostics 101: A Tutorial for Fault Diagnostics of Rolling Element Bearing Using Envelope Analysis in MATLAB. *Applied Sciences*, **10**, Article 7302. https://doi.org/10.3390/app10207302

[8] Ma, M. and Zhu, J. (2024) Interpretable Recurrent Variational State-Space Model for Fault Detection of Complex Systems Based on Multisensory Signals. *Applied Sciences*, **14**, Article 3772. https://doi.org/10.3390/app14093772

[9] Chen, Q., Dong, X., Tu, G., Wang, D., Cheng, C., Zhao, B., *et al.* (2024) TFN: An Interpretable Neural Network with Time-Frequency Transform Embedded for Intelligent Fault Diagnosis. *Mechanical Systems and Signal Processing*, **207**, Article ID: 110952. https://doi.org/10.1016/j.ymssp.2023.110952

[10] Li, Q., Liu, Y., Sun, S., Qin, Z. and Chu, F. (2024) Deep Expert Network: A Unified Method toward Knowledge-Informed Fault Diagnosis via Fully Interpretable Neuro-Symbolic AI. *Journal of Manufacturing Systems*, **77**, 652-661. https://doi.org/10.1016/j.jmsy.2024.10.007

[11] Liu, B., Yan, C., Liu, Y., Wang, Z., Huang, Y. and Wu, L. (2023) Multiscale Residual Antinoise Network via Interpretable Dynamic Recalibration Mechanism for Rolling Bearing Fault Diagnosis with Few Samples. *IEEE Sensors Journal*, **23**, 31425-31439. https://doi.org/10.1109/jsen.2023.3328007

[12] Ho, D. and Randall, R.B. (2000) Optimisation of Bearing Diagnostic Techniques Using Simulated and Actual Bearing Fault Signals. *Mechanical Systems and Signal Processing*, **14**, 763-788. https://doi.org/10.1006/mssp.2000.1304

[13] Shah, J. and Wang, W. (2022) An Evolving Neuro-Fuzzy Classifier for Fault Diagnosis of Gear Systems. *ISA Transactions*, **123**, 372-380.

https://doi.org/10.1016/j.isatra.2021.05.019

[14] Lyu, H.L., Wang, W. and Liu, X.P. (2022) System Identification of Fuzzy Relation Matrix Models by Semi-Tensor Product Operations. *Fuzzy Sets and Systems*, **440**, 77-89. https://doi.org/10.1016/j.fss.2021.06.004

[15] Tian, R., Cui, M.Q. and Chen, G. (2024) A Neural-Symbolic Network for Interpretable Fault Diagnosis of Rolling Element Bearings Based on Temporal Logic. *IEEE Transactions on Instrumentation and Measurement*, **73**, Article ID: 3515614.

[16] Su, X., Deng, C., Shan, Y., Shahnia, F., Fu, Y. and Dong, Z. (2024) Fault Diagnosis Based on Interpretable Convolutional Temporal-Spatial Attention Network for Offshore Wind Turbines. *Journal of Modern Power Systems and Clean Energy*, **12**, 1459-1471. https://doi.org/10.35833/mpce.2023.000606

[17] Gao, S., Zhang, Z., Zhang, X. and Li, H. (2024) WBUN: An Interpretable Convolutional Neural Network with Wavelet Basis Unit Embedded for Fault Diagnosis. *Measurement Science and Technology*, **35**, Article ID: 086125. https://doi.org/10.1088/1361-6501/ad4ab8

[18] Nayana, B.R. and Geethanjali, P. (2017) Analysis of Statistical Time-Domain Features Effectiveness in Identification of Bearing Faults from Vibration Signal. *IEEE Sensors Journal*, **17**, 5618-5625. https://doi.org/10.1109/jsen.2017.2727638

[19] Bertoni, R. and André, H. (2023) Proposition of a Bearing Diagnosis Method Applied to IAS and Vibration Signals: The Bearing Frequency Estimation Method. *Mechanical Systems and Signal Processing*, **187**, Article ID: 109891. https://doi.org/10.1016/j.ymssp.2022.109891

[20] Krishnendu, K. and Pradhan, P.M. (2025) Diagnosis of Bearing Faults Using Optimal Teager-Kaiser Energy Concentrated Time-Frequency Transforms. *IEEE Transactions on Instrumentation and Measurement*, **74**, Article ID: 3516311. https://doi.org/10.1109/tim.2025.3548066

[21] Yu, L., Wang, C., Zhang, F. and Luo, H. (2025) Sparse Time-Frequency Representation via Greedy Method for Diagnosing Bearing Fault under Variable Speed Conditions. *IEEE Transactions on Instrumentation and Measurement*, **74**, Article ID: 3516212. https://doi.org/10.1109/tim.2025.3548179

[22] Wang, W. and Vrbanek, J. (2008) An Evolving Fuzzy Predictor for Industrial Applications. *IEEE Transactions on Fuzzy Systems*, **16**, 1439-1449. https://doi.org/10.1109/tfuzz.2008.925918

[23] Case Western Reserve University (2025) Bearing Data Center. https://engineering.case.edu/bearingdatacenter